CrystEngComm

ROYAL SOCIETY OF CHEMISTRY

PAPER

View Article Online
View Journal | View Issue

Cite this: *CrystEngComm*, 2025, **27**, 1997

Enhanced luminescence in 1D corrugated lead bromides *via* reduced flexibility of trivalent cations†

Chang-Chun Fan, *[a] Zi-Han Fang,[a] Shu-Lin Jiao,[b] Jing-Xue Yu,[a] Cheng-Dong Liu,[b] Wei Wang, *[b] Ming-Liang Jin,[b] Bei-Dou Liang[b] and Xiang-Bin Han *[b]

Received 2nd January 2025,
Accepted 18th February 2025

DOI: 10.1039/d5ce00003c

rsc.li/crystengcomm

Hybrid metal halides (HMHs) have attracted considerable attention from researchers exploring broadband luminescence materials due to their low cost and excellent photophysical properties. Although lots of structures have been developed by researchers based on monovalent and bivalent cations, the importance of trivalent cations in the design of low-dimensional HMH materials with broadband luminescence has been overlooked. In our study, we obtained two new 1D corrugated structures (MPEA)$PbBr_5 \cdot H_2O$ (MPEA is 4-methyl-1-piperazineethanammonium) and $(PEA)_2Pb_2Br_{10} \cdot H_2O$ (PEA is 1-piperazineethanammonium) based on trivalent cations, which can efficiently emit yellow-white light emission with CIE color coordinates of (0.35, 0.42) and (0.42, 0.47) at room temperature with a photoluminescence quantum yield of 0.6% and 10.9%, respectively. Our research underscores the advantages of utilizing low flexible trivalent cations in the development of HMHs with outstanding broadband emission performance and provides novel insight into the design of advanced solid-state luminescent materials.

Introduction

Hybrid metal halides (HMHs) with excellent photophysical properties,[1,2] bandgap tunability,[3] physical stimulus-response behavior,[4] and low cost have shown great competitiveness in the field of optoelectronics, such as solar cells,[5] light emitting diodes,[6] non-volatile memories,[7] lasers,[8,9] photodetectors,[10] and multiferroic devices,[11] and attracted extensive attention from relevant researchers. After nearly a decade of development, researchers have developed a series of HMH semiconductor materials with different structural dimensionalities (quasi-3D, quasi-2D, 2D, 1D, and 0D) using 3D $MAPbI_3$ as a template,[12–18] which has greatly contributed to the development of HMH semiconductors. Particularly, in the field of solid-state luminescence, HMHs can achieve broadband emission of a single component based on the mechanism of self-trapping excitons,[19,20] which makes them the strongest contenders for rare-earth-based solid-state luminescent materials and mixtures of phosphors.[21–23] And, more interesting is that the organic composition, halides and structural dimensionality of HMHs can also be targeted to tune the emission color and polarization state of light.[24–27]

It has been evidenced that the highly localized charge generated by the strong quantum and dielectric confinement effects of HMHs with low structural dimensionality results in structures with higher exciton binding energy and photoluminescence quantum yield (PLQY) than classical 3D HMHs ($MAPbX_3$).[28–30] Therefore, 1D HMHs could be an ideal platform for highly efficient broadband luminescent materials. However, in terms of structure synthesis, organic cations with large structural size or steric resistance are often used,[4,30–33] and there is still a lack of effective strategies to guide the synthesis of corner- or edge-sharing 1D chain structures of metal halide octahedra. Structurally, the flexibility and steric hindrance of organic cations and their interaction with the inorganic framework are important factors affecting the arrangement of inorganic octahedra and dimensionality of HMHs. When the configuration of the cation changes from a highly flexible chain to a less flexible ring, the inorganic anion octahedron will also change the distortion degree and connection mode to adapt to the shape of the cation, further affecting the photophysical properties of the

[a] *School of Materials Engineering, Jinling Institute of Technology, Nanjing 211169, China. E-mail: fcchem@163.com*
[b] *Jiangsu Key Laboratory for Science and Applications of Molecular Ferroelectrics and School of Chemistry and Chemical Engineering, Southeast University, Nanjing 211189, China. E-mail: wangwei96@seu.edu.cn, hanxiangbin.edu@gmail.com*

† Electronic supplementary information (ESI) available: Experimental details, Fig S1–S8 and Table S1–S3. CCDC 2404396 and 2404397. For ESI and crystallographic data in CIF or other electronic format see DOI: **https://doi.org/10.1039/d5ce00003c**

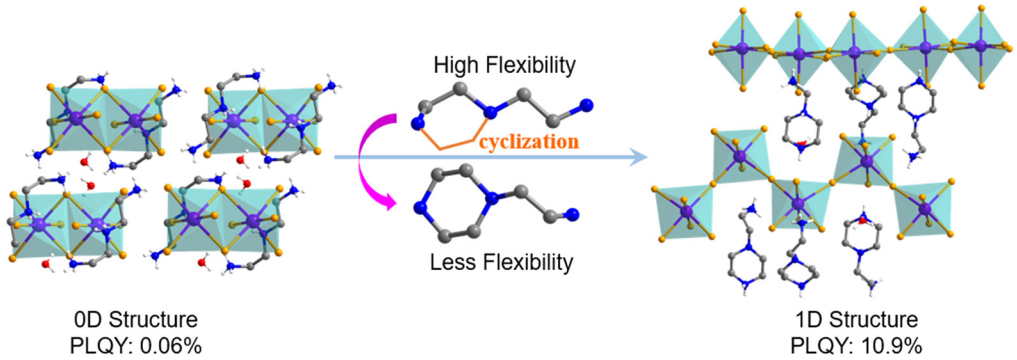

Scheme 1 Illustration of the design of 1D corrugated lead bromide hybrids with broadband luminescence by reducing the flexibility of trivalent cations.

material.[34,35] Multivalent alicyclic cations with certain rigidity, which can not only reduce the dimensionality of the inorganic framework through abundant H···X (X = Cl^-, Br^-, I^-) interactions, but also provide support for inorganic chains through alicyclic rings with relative rigidity, can be ideal template molecules for the synthesis of 1D materials.

In this work, we successfully synthesized two new 1D corrugated structures $(PEA)_2Pb_2Br_{10}\cdot H_2O$ (PEA is 1-piperazineethanammonium) and $(MPEA)PbBr_5\cdot H_2O$ (MPEA is 4-methyl-1-piperazineethanammonium) by reducing the flexibility of trivalent cations with broadband luminescence emission. In particular, the compound $(PEA)_2Pb_2Br_{10}\cdot H_2O$ with adjacent 1D inorganic chains stacked vertically features room-temperature yellowish white-light emission, a high PLQY value of 10.9%, CIE color coordinates of (0.42, 0.47), and correlated color temperatures (CCTs) of

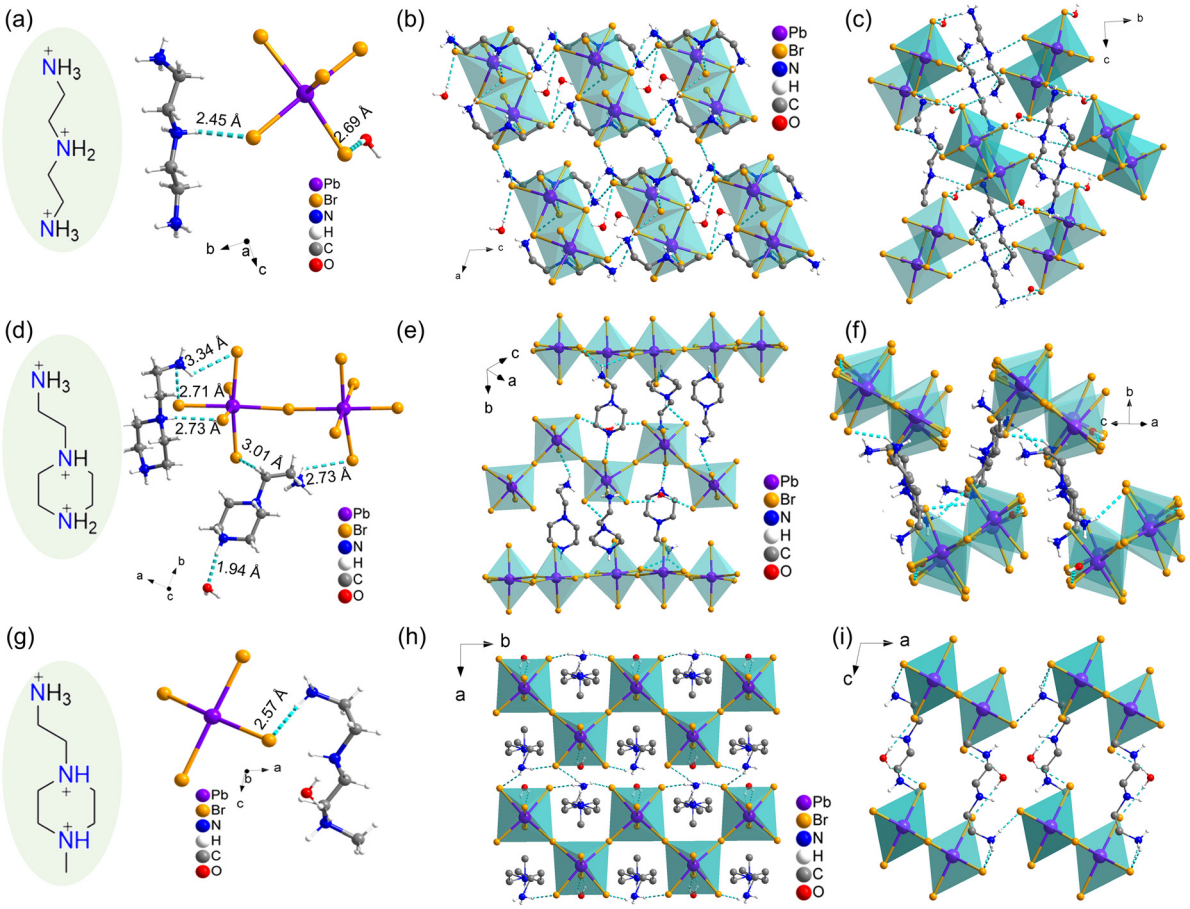

Fig. 1 Asymmetric unit, hydrogen bond interactions between the cation and surroundings, and packing structure of $(DTA)PbBr_5\cdot H_2O$ (a–c), $(PEA)_2Pb_2Br_{10}\cdot H_2O$ (d–f), and $(MPEA)PbBr_5\cdot H_2O$ (g–i) at 298 K. Purple, yellow, blue, gray, and white spheres represent Pb, Br, N, C and H atoms, respectively. Disordered atoms and H atoms are omitted for clarity.

3550 K (Scheme 1). Our research highlights the advantage of trivalent alicyclic cations in the construction of 1D luminescent materials and provides insight into novel broadband optoelectronic devices.

Results and discussion

Synthesis

(DTA)$PbBr_5 \cdot H_2O$ (DTA = diethylenetriammonium). $Pb(Ac)_2$ $3H_2O$ (5.69 g, 15 mmol) was dissolved in 48% HBr solution (80 mL) at 298 K, followed by the addition of 2 mL of 50% H_3PO_2 solution and diethylenetriamine (1.24 g, 15 mmol). The resulting clear solution was evaporated at 328 K. Centimetre-sized white plate-shaped crystals were obtained with a yield of about 40% based on total Pb. The phase purity of the crystals was confirmed by PXRD (Fig. S1a†).[34]

$(PEA)_2Pb_2Br_{10} \cdot H_2O$. $Pb(Ac)_2$ $3H_2O$ (5.69 g, 15 mmol) was dissolved in 48% HBr solution (80 mL) at 298 K, followed by the addition of 2 mL of 50% H_3PO_2 solution and 1-piperazineethanamine (1.73 g, 15 mmol). White precipitates appeared and then were dissolved by heating to 353 K under stirring. The resulting clear solution was evaporated at 328 K. Millimeter-sized light-yellow block-shaped crystals were obtained with a yield of about 60% based on total Pb. Theoretical values for $C_{12}H_{38}Br_{10}N_6OPb_2$: C: 9.64%, H: 2.56%, N: 5.62%. Experimental values: C: 9.76%, H: 2.43%, N: 5.52%. The phase purity of the crystals was confirmed by PXRD (Fig. S1b†).

(MPEA)$PbBr_5 \cdot H_2O$. $Pb(Ac)_2$ $3H_2O$ (5.69 g, 15 mmol) was dissolved in 48% HBr solution (80 mL) at 298 K, followed by the addition of 2 mL of 50% H_3PO_2 solution and 4-methyl-1-piperazineethanamine (1.94 g, 15 mmol). White precipitates appeared and then were dissolved by heating to 353 K under stirring. The resulting clear solution was evaporated at 328 K. Millimeter-sized light-yellow block-shaped crystals were obtained with a yield of about 68% based on total Pb. Theoretical values for $C_7H_{22}Br_5N_3OPb$: C: 10.91%, H: 2.88%, N: 5.45%. Experimental values: C: 11.02%, H: 2.69%, N: 5.31%. The phase purity of the crystals was confirmed by PXRD (Fig. S1c†).

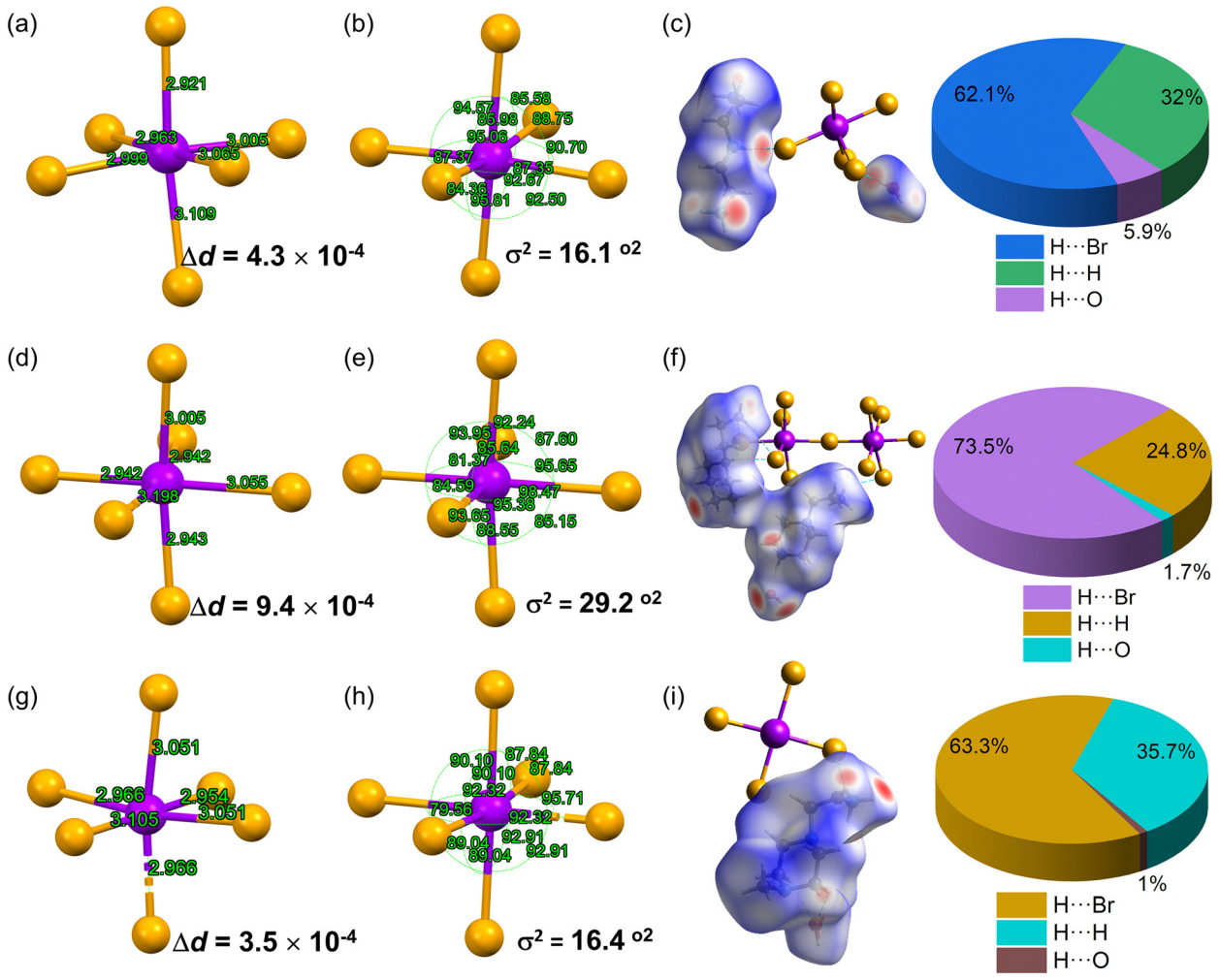

Fig. 2 Distorted $[PbBr_6]$ octahedra and Hirschfeld surface of the cations and H_2O in (DTA)$PbBr_5 \cdot H_2O$ (a–c), $(PEA)_2Pb_2Br_{10} \cdot H_2O$ (d–f), and $(MPEA)_2Pb_2Br_{10} \cdot H_2O$ (g–i) at 298 K.

Crystal structure

(DTA)$PbBr_5 \cdot H_2O$ crystallizes in the centrosymmetric space group $P2_1/c$ at 298 K, and the cell parameters are: a = 10.5210(17) Å, b = 10.7415(16) Å, c = 14.898(2) Å, $\alpha = \gamma = 90°$, and β = 110.020(6)° (Table S1†). The asymmetric unit contains one DTA cation, one Pb ion, five Br ions, and one H_2O molecule (Fig. 1a), the [$PbBr_6$] octahedra are completely isolated and surrounded by DTA and H_2O molecules through H···Br interactions (lengths ranging from 2.45 to 2.69 Å), and the crystal adopts a typical zero-dimensional structure (Fig. 1b and c, and Table S2†). The (DTA)$PbBr_5 \cdot H_2O$ crystals are air and heat stable below 344 K; above that, the crystals first lose crystal water and then gradually decompose (Fig. S2a†).

By cyclization, the highly flexible DTA cation transformed into a less flexible PEA cation, and $(PEA)_2Pb_2Br_{10} \cdot H_2O$ (Fig. 1a) adopts a 1D non-typical corrugated lead-bromide framework (Fig. 1d–f). It crystallizes in the centrosymmetric space group $P2_1/c$ at 298 K, and the cell parameters are: a = 13.8538(3) Å, b = 17.5673(3) Å, c = 13.8398(3) Å, $\alpha = \gamma = 90°$, and β = 96.191(2)° (Fig. 1 and Table S1†). The 1D chain is composed of corner-sharing [$PbBr_6$] octahedra. The octahedra are arranged in a corrugated pattern in the (101) direction, with a pocket in the middle of the three adjacent octahedra stabilized by H···Br interactions among cations, H_2O, and bromine ions (Fig. 1d and f and Table S2†). The H_2O molecule is in the pocket formed by the octahedron, not between inorganic chains, which results in a 43 K increase in the thermal stability of the crystal compared to (DTA)$PbBr_5 \cdot H_2O$ (Fig. S2b†). It also differs from the general 1D structure in crystal stacking, where the adjacent inorganic chains are not stacked in parallel, but almost vertically. This could improve the performance of materials based on the self-trapping exciton luminescence mechanism. In contrast to $(PEA)_2Pb_2Br_{10} \cdot H_2O$, (MPEA)$PbBr_5 \cdot H_2O$ retains a similar corrugated inorganic framework (Fig. 1g–i), but the H_2O molecules move from the pocket within the inorganic chain to the inorganic interchain, greatly reducing its structural thermal stability.

In order to further evaluate the influence of cation changes on the microstructure of the inorganic framework, we studied the distortion of [$PbBr_6$]. Two parameters, Δd and σ^2, reflecting the bond length distortion and bond angle variance, respectively, were calculated using the following expressions

$$\Delta d = \left(\frac{1}{6}\right)\sum_{i=1}^{6}\frac{(d_i - d_o)^2}{{d_o}^2}$$

$$\sigma^2 = \left(\frac{1}{11}\right)\sum_{i=1}^{12}(\theta_i - 90)^2$$

where d_o and d_i are the average and individual Pb–Br bond distance, respectively, and θ_i is the angle of the individual Br–Pb–Br angle. In the (DTA)$PbBr_5 \cdot H_2O$ structure synthesized from flexible cations, the Pb–Br bond lengths vary between 2.921 and 3.109 Å with a distortion parameter Δd of 4.3 × 10^{-4} (Fig. 2a), which is comparable to 1D chiral HMHs (R/S-3-OHPD)PbI_3 (ref. 36) and 2D chiral ferroelectric (R/S-3AMP)$PbBr_4$.[37] At the same time, the bond angles vary between 84.36 and 95.81° with a distortion parameter σ^2 of 16.1° (ref. 2) (Fig. 2b and Table S3†). In the (PEA)$PbBr_5 \cdot H_2O$ structure synthesized from rigid cations, Δd and σ^2 are approximately doubled compared to those of (DTA)$PbBr_5 \cdot H_2O$, reaching 9.4 × 10^{-4} and 29.0° (ref. 2) (Fig. 2d and e and Table S3†), respectively. The increase of cation rigidity not only changes the dimensionality of the inorganic anion skeleton, but also greatly increases the degree of distortion of the inorganic octahedron. Hirshfeld surface analysis also showed that the enhancement of cation rigidity enhanced the H···Br interaction among organic cations, H_2O and inorganic anions, and weakened the interaction between cation molecules (Fig. 2c and f and S3 and S4†), which was consistent with the change of the structural dimensionality (Fig. 1b and e). After further methylation of the secondary amine end of the PEA cation to the tertiary amine, it is found that although the inorganic framework maintains the 1D corrugated structure, the distortion of the [$PbBr_6$] and H···Br interaction is greatly reduced (Fig. 2g–i and S5†), which is

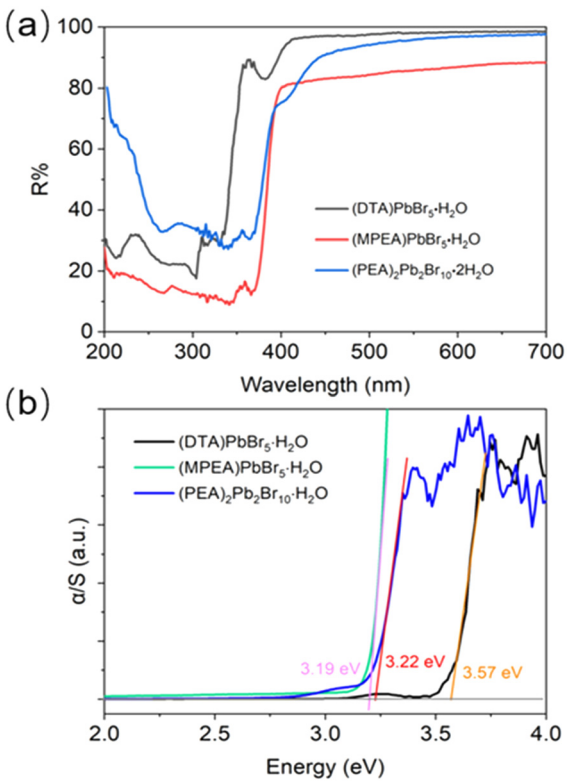

Fig. 3 UV-vis diffuse-reflectance spectra (a) and bandgaps derived from the Kubelka–Munk function (b) of (DTA)$PbBr_5 \cdot H_2O$, $(PEA)_2Pb_2Br_{10} \cdot H_2O$, and $(MPEA)_2Pb_2Br_{10} \cdot H_2O$.

comparable to the 0D structure. This suggests that rigid cations help improve the structural dimensionality of HMHs, while tertiary amines are not a good template for increasing the interaction of cations with inorganic frameworks.

Semiconducting and photoluminescence properties

The photophysical properties of the targeted compounds were characterized by using ultraviolet-visible diffuse reflectance spectroscopy and steady-state time-resolved PL spectroscopy. The band gap estimated by the Kubelka–Munk function is 3.57 eV for (DTA)$PbBr_5 \cdot H_2O$, 3.22 eV for $(PEA)_2Pb_2Br_{10} \cdot H_2O$, and 3.19 eV for (MPEA)$PbBr_5 \cdot H_2O$ (Fig. 3a and b). There is a significant redshift in the band gap (Fig. 3b), which is consistent with the changes in structural dimensionality and [$PbBr_6$] octahedral distortion (Fig. 2).[27]

Consequently, the PL properties of the targeted compounds were studied, and all the compounds exhibit broadband emission from the STE mechanism.[38] Under 325 nm excitation, (DTA)$PbBr_5 \cdot H_2O$ shows broadband orange emission, which is invisible to the naked eye and corresponds to a weak quantum yield (Fig. 4a and S6†). $(PEA)_2Pb_2Br_{10} \cdot H_2O$ emits brighter yellowish light that covers the visible light range with a full width at half-maximum (FWHM) exceeding 184 nm (Fig. 4b), under 365 nm excitation. The international chromaticity coordinates of (0.42, 0.47) represent yellow emission (Fig. 4d). The PLQY and average luminescence lifetime are 10.9% and 23.8 ns, respectively (Fig. 4e and h), which are much higher than those of 1D chiral HMH (*R*/*S*-3-OHPD)PbI_3.[36] (MPEA) $PbBr_5 \cdot H_2O$ emits yellowish white-light with CIE coordinates of (0.35, 0.42) (Fig. 4d), but the brightness, PLQY, and average luminescence lifetime are significantly reduced (Fig. 4c, f and i). From the above PL data, we found that the emission wavelength of the 1D structure is blue-shifted compared with that of the 0D structure (Fig. 4g), and the vertical stacking between chains in the 1D structure has better optical performance than the parallel stacking. In addition, since the structure contains a solvent of crystallization, there may be a phenomenon of fluorescence changes caused by the loss of solvent of crystallization.[39–41] We further investigated the

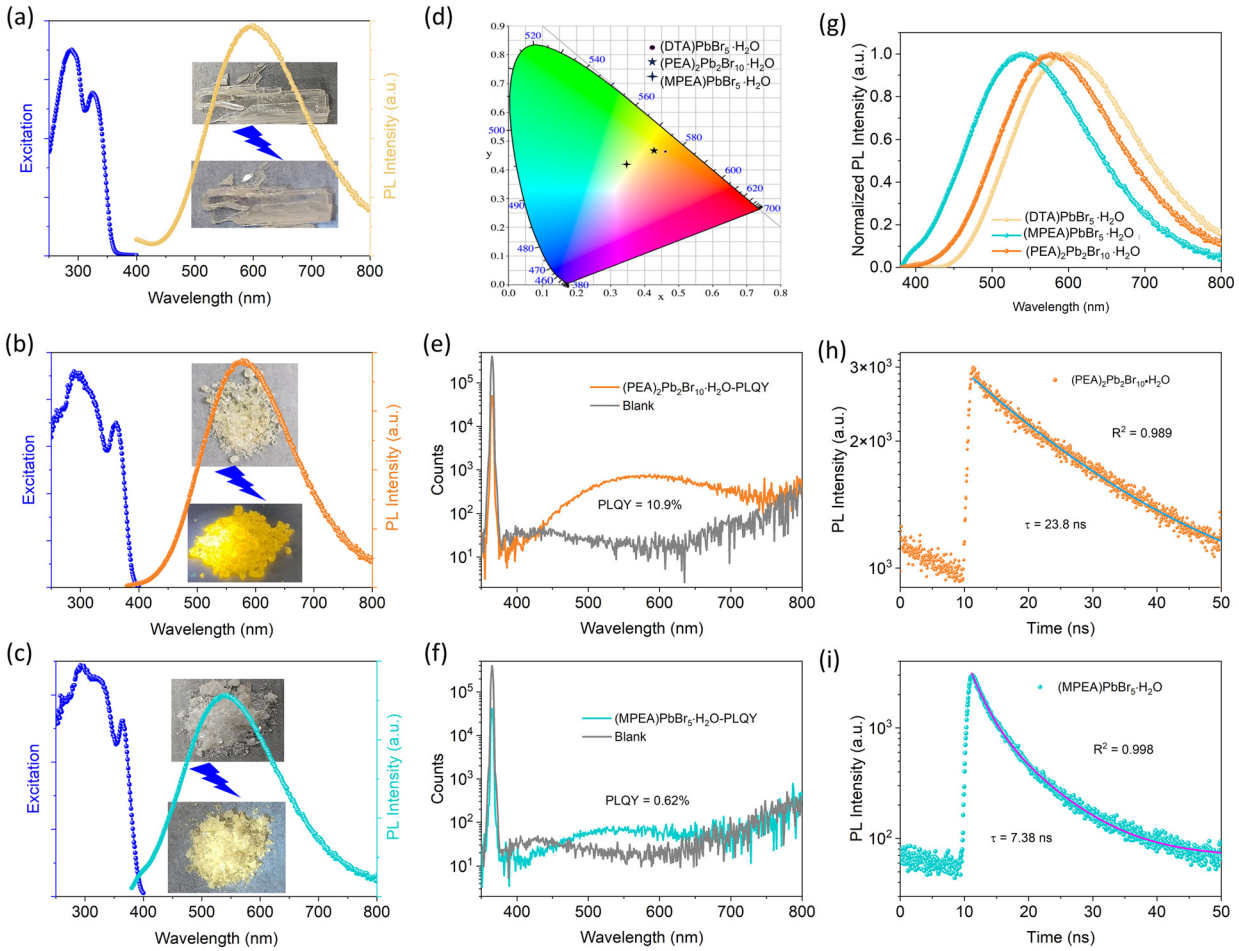

Fig. 4 Photoluminescence spectra of (DTA)$PbBr_5 \cdot H_2O$ (a), $(PEA)_2Pb_2Br_{10} \cdot H_2O$ (b), and (MPEA)$_2Pb_2Br_{10} \cdot H_2O$ (c). (d) CIE chromaticity coordinates. (g) Comparison of fluorescence emission wavelengths. PLQY and luminescence decays of $(PEA)_2Pb_2Br_{10} \cdot H_2O$ (e and h) and (MPEA)$PbBr_5 \cdot H_2O$ (f and i) at 298 K.

fluorescence properties after the dehydration of the structure. $(PEA)_2Pb_2Br_{10}\cdot H_2O$ shows a slight redshift in the fluorescence spectrum (4 nm) after the loss of water of crystallization, with a decrease in PLQY of 1.36% (Fig. S4a–c†). Meanwhile $(MPEA)PbBr_5\cdot H_2O$ shows a large redshift in the fluorescence spectrum of 77 nm after the loss of water of crystallization, with an increase in PLQY of 0.32% (Fig. S4e and f†). The above phenomena further indicate that the fluorescence properties of the materials originate from the inorganic backbone. In addition, the crystals can return to the initial state by regaining water molecules after losing them (Fig. S8†), showing potential applications in the field of chemical sensors and solid-state luminescent materials.

Conclusions

In conclusion, we constructed two new 1D corrugated structures $(PEA)_2Pb_2Br_{10}\cdot H_2O$ and $(MPEA)PbBr_5\cdot H_2O$ with broadband emission by the strategy of reducing the flexibility of trivalent cations. In particular, the compound $(PEA)_2Pb_2Br_{10}\cdot H_2O$ with inorganic chains alternately stacked vertically along the *b* direction features room-temperature yellow-white light emission and a high photoluminescence quantum yield (PLQY) value of 10.9%, which make it a promising light emitter in optoelectronic devices. Our research highlights the advantage of less flexible multi-valent cations in the construction of 1D luminescent materials and a new platform for fundamental studies of the structure–property relationships in broadband luminescent systems.

Data availability

The data supporting this article have been included as part of the ESI.†

Author contributions

Chang-Chun Fan: conceptualization, data curation, funding acquisition, formal analysis, methodology, validation and writing – original draft; Zi-Han Fan: data curation and investigation; Shu-Lin Jiao: investigation and methodology; Jing-Xue Yu: supervision; Cheng-Dong Liu: data curation and methodology; Wei Wang: investigation and writing – review & editing; Ming-Liang Jin: formal analysis; Bei-Dou Liang: visualization and formal analysis; Xiang-Bin Han: conceptualization, funding acquisition, resources, supervision and writing – review & editing.

Conflicts of interest

There are no conflicts to declare.

Acknowledgements

This work was financially supported by the Talent Introduction Project of Jinling Institute of Technology (JIT-B-202414) and the Natural Science Foundation of Jiangsu Province (Grant No. BK20230811).

References

1 B. R. Sutherland and E. H. Sargent, *Nat. Photonics*, 2016, **10**, 295–302.
2 J. Lim, M. T. Hörantner, N. Sakai, J. M. Ball, S. Mahesh, N. K. Noel, Y.-H. Lin, J. B. Patel, D. P. McMeekin, M. B. Johnston, B. Wenger and H. J. Snaith, *Energy Environ. Sci.*, 2019, **12**, 169–176.
3 H. Y. Ye, W. Q. Liao, C. L. Hu, Y. Zhang, Y. M. You, J. G. Mao, P. F. Li and R. G. Xiong, *Adv. Mater.*, 2016, **28**, 2579–2586.
4 B. D. Liang, C. C. Fan, C. D. Liu, C. Y. Chai, X. B. Han and W. Zhang, *Nat. Commun.*, 2022, **13**, 6599.
5 S. Li, Y. Jiang, J. Xu, D. Wang, Z. Ding, T. Zhu, B. Chen, Y. Yang, M. Wei, R. Guo, Y. Hou, Y. Chen, C. Sun, K. Wei, S. M. H. Qaid, H. Lu, H. Tan, D. Di, J. Chen, M. Grätzel, E. H. Sargent and M. Yuan, *Nature*, 2024, **635**, 82–88.
6 Y. H. Kim, Y. X. Zhai, H. P. Lu, X. Pan, C. X. Xiao, E. A. Gaulding, S. P. Harvey, J. J. Berry, Z. V. Vardeny, J. M. Luther and M. C. Beard, *Science*, 2021, **371**, 1129–1133.
7 H. Xu, F. Sun, E. Li, W. Guo, L. Hua, R. Wang, W. Li, J. Chu, W. Liu, J. Luo and Z. Sun, *Adv. Mater.*, 2024, **36**, 2414339.
8 J. Cheng, G. Yi, Z. Zhang, Y. Long, H. Zeng, L. Huang, G. Zou and Z. Lin, *Angew. Chem., Int. Ed.*, 2024, **63**, e202318385.
9 H. Zhu, Y. Fu, F. Meng, X. Wu, Z. Gong, Q. Ding, M. V. Gustafsson, M. T. Trinh, S. Jin and X. Y. Zhu, *Nat. Mater.*, 2015, **14**, 636–642.
10 J. Feng, C. Gong, H. Gao, W. Wen, Y. Gong, X. Jiang, B. Zhang, Y. Wu, Y. Wu, H. Fu, L. Jiang and X. Zhang, *Nat. Electron.*, 2018, **1**, 404–410.
11 M.-L. Jin, X.-B. Han, C.-D. Liu, C.-Y. Chai, C.-Q. Jing, W. Wang, C.-C. Fan, J.-M. Zhang and W. Zhang, *J. Am. Chem. Soc.*, 2024, **146**, 6336–6344.
12 X. Li, J. M. Hoffman and M. G. Kanatzidis, *Chem. Rev.*, 2021, **121**, 2230–2291.
13 P. Siwach, P. Sikarwar, J. S. Halpati and A. K. Chandiran, *J. Mater. Chem. A*, 2022, **10**, 8719–8738.
14 H. P. Wang, S. Li, X. Liu, Z. Shi, X. Fang and J. H. He, *Adv. Mater.*, 2020, **32**, 2003309.
15 C.-C. Fan, C.-D. Liu, B.-D. Liang, T.-Y. Ju, W. Wang, M.-L. Jin, C.-Y. Chai and W. Zhang, *Chem. Sci.*, 2024, **15**, 11374–11381.
16 W. Wang, C.-D. Liu, C.-C. Fan and W. Zhang, *Chem. Sci.*, 2024, **15**, 18455–18462.
17 C.-C. Fan, B.-D. Liang, C.-D. Liu, C.-Y. Chai, X.-B. Han and W. Zhang, *Inorg. Chem. Front.*, 2022, **9**, 6404–6411.
18 W. Wang, C.-D. Liu, C.-C. Fan, X.-B. Fu, C.-Q. Jing, M.-L. Jin, Y.-M. You and W. Zhang, *J. Am. Chem. Soc.*, 2024, **146**, 9272–9284.
19 L. N. Quan, J. Kang, C.-Z. Ning and P. Yang, *Chem. Rev.*, 2019, **119**, 9153–9169.

20 X.-B. Han, C.-Q. Jing, H.-Y. Zu and W. Zhang, *J. Am. Chem. Soc.*, 2022, **144**, 18595–18606.
21 S. Ye, F. Xiao, Y. X. Pan, Y. Y. Ma and Q. Y. Zhang, *Mater. Sci. Eng., R*, 2010, **71**, 1–34.
22 J. Zhang, L. Wang, A. Zhong, G. Huang, F. Wu, D. Li, M. Teng, J. Wang and D. Han, *Dyes Pigm.*, 2019, **162**, 590–598.
23 Z. Liu, X. Li, W. Dai, J.-J. Liu and M.-J. Lin, *Coord. Chem. Rev.*, 2025, **526**, 216350.
24 C. Y. Chai, Q. K. Zhang, C. Q. Jing, X. B. Han, C. D. Liu, B. D. Liang, C. C. Fan, Z. Chen, X. W. Lei, A. Stroppa, R. O. Agbaoye, G. A. Adebayo, C. F. Zhang and W. Zhang, *Adv. Opt. Mater.*, 2022, **11**, 2201996.
25 K. H. Jin, Y. Zhang, K. J. Li, M. E. Sun, X. Y. Dong, Q. L. Wang and S. Q. Zang, *Angew. Chem., Int. Ed.*, 2022, **61**, e202205317.
26 H. Y. Zu, X. B. Han, C. C. Fan, B. D. Liang and W. Zhang, *lnorg. Chem*, 2022, **61**, 17738–17745.
27 H.-Y. Zu, C.-C. Fan, C.-D. Liu, C.-Q. Jing, C.-Y. Chai, B.-D. Liang, X.-B. Han and W. Zhang, *Chem. Mater.*, 2023, **35**, 5854–5863.
28 J. Zhou, M. Li, L. Ning, R. Zhang, M. S. Molokeev, J. Zhao, S. Yang, K. Han and Z. Xia, *J. Phys. Chem. Lett.*, 2019, **10**, 1337–1341.
29 G.-E. Wang, G. Xu, M.-S. Wang, L.-Z. Cai, W.-H. Li and G.-C. Guo, *Chem. Sci.*, 2015, **6**, 7222–7226.
30 L. Mao, P. Guo, M. Kepenekian, I. Hadar, C. Katan, J. Even, R. D. Schaller, C. C. Stoumpos and M. G. Kanatzidis, *J. Am. Chem. Soc.*, 2018, **140**, 13078–13088.
31 V. Gomez, O. Fuhr and M. Ruben, *CrystEngComm*, 2016, **18**, 8207–8219.
32 R. Chen, C. Sun, X. Cheng, Y. Lin, J. Zhou, J. Yin, B. B. Cui and L. Mao, *Inorg. Chem.*, 2023, **62**, 9722–9731.
33 C.-C. Gao, X.-N. Tang, J.-L. Miao, Y. Li, C. Li and G.-N. Liu, *CrystEngComm*, 2023, **25**, 6556–6567.
34 A. Yangui, R. Roccanova, Y. T. Wu, M. H. Du and B. Saparov, *J. Phys. Chem. C*, 2019, **123**, 22470–22477.
35 Y. L. Zeng, X. Q. Huang, C. R. Huang, H. Zhang, F. Wang and Z. X. Wang, *Angew. Chem., Int. Ed.*, 2021, **60**, 10730–10735.
36 M. L. Jin, X. B. Han, C. D. Liu, B. D. Liang, C. Q. Jing, W. Wang, C. C. Fan, T. Y. Ju, J. M. Zhang and W. Zhang, *Adv. Funct. Mater.*, 2024, **34**, 2408120.
37 C. C. Fan, X. B. Han, B. D. Liang, C. Shi, L. P. Miao, C. Y. Chai, C. D. Liu, Q. Ye and W. Zhang, *Adv. Mater.*, 2022, **34**, 2204119.
38 W. Wang, C.-D. Liu, X.-B. Han, C.-Q. Jing, C.-Y. Chai, C.-C. Fan, M.-L. Jin, J.-M. Zhang and W. Zhang, *ACS Mater. Lett.*, 2024, **6**, 203–211.
39 S. A. Adonin, M. E. Rakhmanova, A. I. Smolentsev, I. V. Korolkov, M. N. Sokolov and V. P. Fedin, *New J. Chem.*, 2015, **39**, 5529–5533.
40 S. A. Adonin, M. N. Sokolov, M. E. Rakhmanova, A. I. Smolentsev, I. V. Korolkov, S. G. Kozlova and V. P. Fedin, *Inorg. Chem. Commun.*, 2015, **54**, 89–91.
41 D. Yan, G. Fan, Y. Guan, Q. Meng, C. Li and J. Wang, *Phys. Chem. Chem. Phys.*, 2013, **15**, 19845–19852.